Intermittent Hypoxia Triggers Early Cardiac Remodeling and Contractile Dysfunction in the Time-Course of Ischemic Cardiomyopathy in Rats

Guillaume Bourdier, Maximin Détrait, Sophie Bouyon, Emeline Lemarié, Sandrine Brasseur, Stéphane Doutreleau, Jean-louis Pépin, Diane Godin-Ribuot, Elise Belaidi, Claire Arnaud

▶ **To cite this version:**

Guillaume Bourdier, Maximin Détrait, Sophie Bouyon, Emeline Lemarié, Sandrine Brasseur, et al.. Intermittent Hypoxia Triggers Early Cardiac Remodeling and Contractile Dysfunction in the Time-Course of Ischemic Cardiomyopathy in Rats. Journal of the American Heart Association, 2020, 9 (16), pp.e016369. 10.1161/JAHA.120.016369 . inserm-03807172

HAL Id: inserm-03807172

https://inserm.hal.science/inserm-03807172

Submitted on 9 Oct 2022

HAL is a multi-disciplinary open access archive for the deposit and dissemination of scientific research documents, whether they are published or not. The documents may come from teaching and research institutions in France or abroad, or from public or private research centers.

L'archive ouverte pluridisciplinaire **HAL**, est destinée au dépôt et à la diffusion de documents scientifiques de niveau recherche, publiés ou non, émanant des établissements d'enseignement et de recherche français ou étrangers, des laboratoires publics ou privés.

Journal of the American Heart Association

ORIGINAL RESEARCH

Intermittent Hypoxia Triggers Early Cardiac Remodeling and Contractile Dysfunction in the Time-Course of Ischemic Cardiomyopathy in Rats

Guillaume Bourdier, PhD*; Maximin Détrait, MSc*; Sophie Bouyon, MSc; Emeline Lemarié, MSc; Sandrine Brasseur, BSc; Stéphane Doutreleau, MD, PhD; Jean-Louis Pépin, MD, PhD; Diane Godin-Ribuot, PhD; Elise Belaidi, PhD†; Claire Arnaud, PharmD, PhD†

BACKGROUND: Sleep-disordered breathing is associated with a poor prognosis (mortality) in patients with ischemic cardiomyopathy. The understanding of mechanisms linking intermittent hypoxia (IH), the key feature of sleep-disordered breathing, to ischemic cardiomyopathy progression is crucial for identifying specific actionable therapeutic targets. The aims of the present study were (1) to evaluate the impact of IH on the time course evolution of cardiac remodeling and contractile dysfunction in a rat model of ischemic cardiomyopathy; and (2) to determine the impact of IH on sympathetic activity, hypoxia inducible factor-1 activation, and endoplasmic reticulum stress in the time course of ischemic cardiomyopathy progression.

METHODS AND RESULTS: Ischemic cardiomyopathy was induced by a permanent ligature of the left coronary artery in male Wistar rats (rats with myocardial infarction). Rats with myocardial infarction were then exposed to either IH or normoxia for up to 12 weeks. Cardiac remodeling and function were analyzed by Sirius red and wheat germ agglutinin staining, ultrasonography, and cardiac catheterization. Sympathetic activity was evaluated by spectral analysis of blood pressure variability. Hypoxia-inducible factor-1α activation and burden of endoplasmic reticulum stress were characterized by Western blots. Long-term IH exposure precipitated cardiac remodeling (hypertrophy and interstitial fibrosis) and contractile dysfunction during the time course evolution of ischemic cardiomyopathy in rodents. Among associated mechanisms, we identified the early occurrence and persistence of sympathetic activation, associated with sustained hypoxia-inducible factor-1α expression and a delayed pro-apoptotic endoplasmic reticulum stress.

CONCLUSIONS: Our data provide the demonstration of the deleterious impact of IH on post–myocardial infarction remodeling and contractile dysfunction. Further studies are needed to evaluate whether targeting sympathetic nervous system or HIF-1 overactivities could limit these effects and improve management of coexisting ischemic cardiomyopathy and sleep-disordered breathing.

Key Words: ER stress ■ hypoxia inducible factor-1 ■ intermittent hypoxia ■ ischemic cardiomyopathy ■ sleep-disordered breathing ■ sympathetic activation

Downloaded from http://ahajournals.org by on October 13, 2022

Coronary artery disease, and especially acute coronary syndrome (ACS), is the leading cause of death in industrialized countries and develops because of complex interactions between multiple risk factors and comorbidities.[1] ACS is defined as unstable angina, non–ST-segment elevation myocardial

Correspondence to: Claire Arnaud, PharmD, PhD, Laboratoire HP2, Université Grenoble Alpes, INSERM U1042, Place du Commandant Nal, Faculté de Médecine de Grenoble, 38700 La Tronche, France. E-mail: claire.arnaud@univ-grenoble-alpes.fr

*Dr Bourdier and Mr Détrait are co-first authors.

†Dr Belaidi and Dr Arnaud are co-senior authors.

For Sources of Funding and Disclosures, see page 12.

© 2020 The Authors. Published on behalf of the American Heart Association, Inc., by Wiley. This is an open access article under the terms of the Creative Commons Attribution-NonCommercial-NoDerivs License, which permits use and distribution in any medium, provided the original work is properly cited, the use is non-commercial and no modifications or adaptations are made.

JAHA is available at: www.ahajournals.org/journal/jaha

CLINICAL PERSPECTIVE

What Is New?

- Long-term exposure to intermittent hypoxia precipitates cardiac remodeling (hypertrophy and interstitial fibrosis) and contractile dysfunction during the time course evolution of ischemic cardiomyopathy in rodents.
- We identified early occurrence of sustained sympathetic activation, sustained hypoxia-inducible factor-1α expression, and delayed pro-apoptotic endoplasmic reticulum stress following intermittent hypoxia exposure.

What Are the Clinical Implications?

- This study describes different steps of cardiac function deterioration after myocardial infarction and associated mechanisms induced by intermittent hypoxia, the hallmark feature of sleep-disordered breathing.
- Further studies are needed to evaluate whether targeting intermittent hypoxia-induced sympathetic nervous system, hypoxia-inducible factor-1 overactivity could limit these effects and improve management of co-existing ischemic cardiomyopathy and sleep-disordered breathing.

Nonstandard Abbreviations and Acronyms

ACS	acute coronary syndrome
CPAP	continuous positive airway pressure
ER	endoplasmic reticulum
HIF	hypoxia-inducible factor
IH	intermittent hypoxia
LV	left ventricle
MI	myocardial infarction
N	normoxia
SDB	sleep-disordered breathing
SNS	sympathetic nervous system

infarction and ST-segment–elevation myocardial infarction[2] and contributes to heart failure progression.[3] Sleep-disordered breathing (SDB) is recognized as an independent cardiovascular risk factor,[4] is highly prevalent (up to 60%) in patients with ACS,[5] and is associated with a higher rate of death in heart failure.[6] In the early phase after myocardial infarction (MI), SDB promotes infarct expansion, reduces myocardial salvage, and impairs ventricular remodeling.[7] In addition, in a cohort of patients hospitalized for ACS, SDB is associated with higher peak troponin levels in plasma, increased number of diseased vessels, and duration of hospitalization period.[8] The understanding of mechanisms linking intermittent hypoxia (IH), the key feature of SDB, to ischemic cardiomyopathy progression is crucial for identifying specific actionable therapeutic targets.

IH has been identified as the key mediator for deleterious cardiovascular impact of SDB.[9] In rodent models, IH induces an increase in infarct size in response to acute myocardial ischemia–reperfusion.[10–12] However, the role of IH in the long-term progression of chronic ischemic cardiomyopathy remains to be established. Studies in rodents emphasized that IH triggers a chronic and sustained sympathetic nervous system (SNS) activity,[12–14] increases hypoxia-inducible factor (HIF)-1 activity, and enhances myocardial pro-apoptotic endoplasmic reticulum (ER) stress[11,15–17]. Individually, all these mechanisms have been demonstrated to be closely related to the IH-induced increase in infarct size,[11,12] cardiomyocytes apoptosis, and left ventricular (LV) dysfunction.[12,15,16,18] These IH-induced pathogenic mechanisms may also play an aggravating role in the progression of chronic ischemic cardiomyopathy.

The originality of the current study was to use a long-term time course experimental design to (1) evaluate the impact of IH on cardiac remodeling and contractile dysfunction in a rat model of chronic ischemic cardiomyopathy; and (2) to determine the impact of IH on sympathetic activity, HIF-1 activation, and ER stress in the time course of ischemic cardiomyopathy progression.

METHODS

The data, methods used in the analysis, and materials used to conduct the study are available from the corresponding author upon reasonable request.

Study Population

Wistar male rats (5-week-old, 200–220 g, Janvier Labs, Le Genest-Saint-Isle, France) were housed at the animal care facility of the HP2 Laboratory (approval no. A38 51610006) under a 12:12 hours light–dark cycle at 20°C to 22°C and allowed free access to standard food and water. The experimental procedures were conducted in accordance with the European Convention for the Protection of Vertebrate Animals used for Experimental and Other Scientific Purposes (Council of Europe, European Treaties ETS 123, Strasbourg, 18 March 1986) and with the Guide for Care and Use of Laboratory Animals (NIH Publication No. 85-23, revised 1996) and were approved by an Institutional Animal Care and Use Committee (agreement number 2015032010109170 (APAFIS#695)).

Downloaded from http://ahajournals.org by on October 13, 2022

Myocardial Infarction

Six-week-old rats were anesthetized (ketamine (100 mg/kg ip; Imalgene 1000, Merial, France) and xylazine (4 mg/kg ip; Rompun, Bayer, Germany), intubated, and ventilated in a 50% O_2 –50% air mixture on a volume control ventilator (Rovent; Kent Scientific, Torrington, Connecticut). Anesthesia was maintained with 0.5% isoflurane (Isoflo; Axience, Pantin, France) in a 50% O_2 –50% air mixture during the procedure. Respiratory rate, tidal volume (Kent Scientific), and expired CO_2 (Capnoscan, Kent Scientific) were monitored. Rat temperature was regulated using a rectal probe connected to a heating pad. Following a left thoracotomy, the pericardium was dissected, and the left anterior coronary artery was ligated using a nonabsorbable braided silk suture (sofsilk 6-0; Covidien, Boulogne-Billancourt, France). The rib cage was closed and the wound sutured (polysorb 4-0, Covidien). Sham-operated rats were subjected to the same surgical procedure except for the coronary artery ligation. All animals were given 0.03 mg/kg buprenorphine (Buprécare; Axience) subcutaneously immediately after surgery.

Echocardiography (2D and M-mode) was performed 3 days after surgery to exclude animals with small infarcts and limited reduction of LV ejection fraction (>45%) according to the procedure described by Litwin et al.[19] Regarding the 75 rats operated on, all the sham rats survived, 9 rats with MI died (11%) during the first 24 hours, and 10 (12%) were excluded for left ventricular ejection fraction >45% (Figure 1). The infarcted rats were matched according to their left ventricular ejection fraction values in 2 homogeneous groups (MI-normoxia [N] and MI-IH), infarct size reproducibility was confirmed postmortem, and 1 MI-IH rat was excluded for too-small infarct size.

Intermittent Hypoxia

Rats were randomly exposed to IH or N for 4–12 weeks (Figure 1), in our HypE platform (https://hp2.univ-grenoble-alpes.fr/plateforme-hypeGrenoble, France). Animals were exposed daily to 8 hours of IH or N during their daytime sleep period. The IH stimulus was performed using a specifically designed device, as previously described.[20] It consisted of 1-minute cycles with alternating 30 seconds of hypoxia (5% fraction of inspired O_2 (FiO_2) and 30 seconds of normoxia (21% FiO_2). FiO_2 was monitored throughout the experiment with a gas analyzer (ML206; AD Instruments, Oxford, UK). Normoxic rats were exposed to air streams to reproduce equivalent levels of noise and turbulence related to gas circulation. Sham rats were maintained in housing cages. At the end of exposure, rats were anesthetized with injection of ketamine (100 mg/kg ip, Merial) and xylazine (4 mg/kg ip, Bayer) before experimental procedures.

Echocardiography

A longitudinal follow-up of rat LV dimensions and function was performed weekly and every 2 weeks for 4- and 12-week exposure, respectively. Rats were anesthetized with 5% isoflurane (Axience) in a 50% O_2

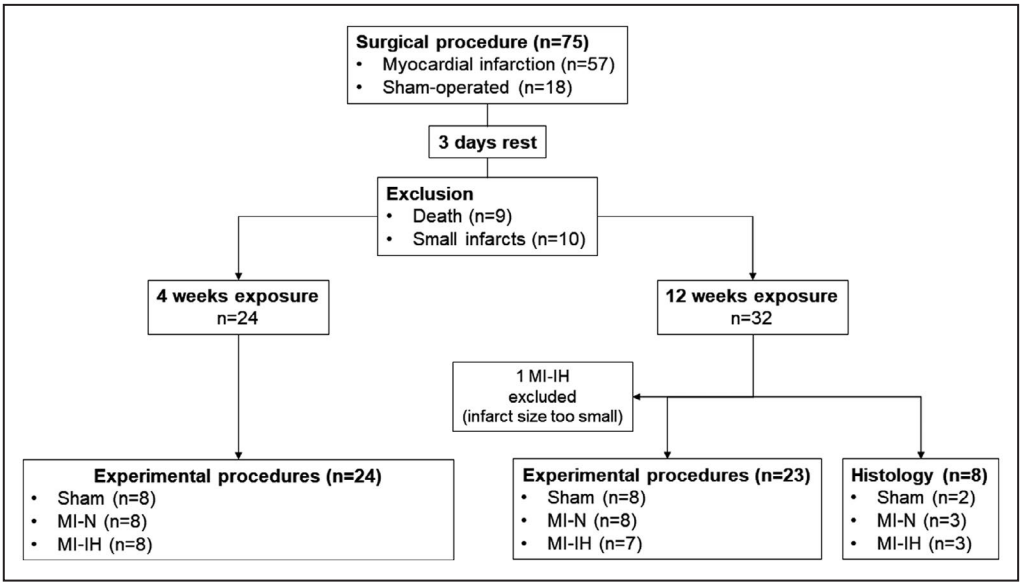

Figure 1. Study flow chart. Rats underwent a ligature of the left coronary artery to induce myocardial infarction (MI) or a sham surgery (Sham).
Three days after coronary artery ligation, rats with MI were randomly exposed to 4- or 12-weeks intermittent hypoxia (IH) or normoxia (N). At the end of exposures, rats were anesthetized for experimental procedures (power spectral analysis of arterial blood pressure variability, pressure-volume loop analysis) and tissues were harvested for histology or molecular biology.

Downloaded from http://ahajournals.org by on October 13, 2022

–50% air mixture and maintained with 2% isoflurane during the procedure. Using an ultra-high-frequency probe (MS250 13–24 MHz, VisualSonics), diastolic and systolic LV wall thickness, cavity diameter, and ejection fraction were measured and calculated as the mean of 3 cardiac cycles in M-mode long axis.

Histology

An intracardiac injection of KCl 120 mmol/L stopped rat hearts in diastolic phase. Hearts and adrenal glands were harvested and fixed overnight in 4% paraformaldehyde in PBS and were embedded in paraffin. Five-micrometer sections (RM2255 Fully Automated Rotary Microtome, Leica) were stained for 1 hour with Sirius-red (0.1% of Sirius red in saturated picric acid) and washed twice with acidified water. Interstitial fibrosis density in remote areas of the infarct was determined through ImageJ analysis.

Wheat germ agglutinin Oregon Green 488 conjugate (Molecular Probes) was used in order to measure cardiomyocytes minimum Feret diameter (μm) at a 1/100 dilution for 1 hour. Cross-sectional area analysis was performed using a macro in ImageJ (*Stochastic watershed* plugin, adapted by Dr A. Fertin, TIMC-IMAG).

Apoptosis was determined through analysis of DNA fragmentation by terminal deoxynucleotidyl transferase-mediated dUTP nick end-labeling (TUNEL) assay on paraffin-embedded sections, following the manufacturer's instruction (Abcam, Cambridge, United Kingdom) as previously described.[21] An Axioscan fluorescent microscope (Zeiss, Göttingen, Germany, ×20) was used to visualize TUNEL-positive red cells and sections were counterstained with 4′,6-diamidino-2-phenylindole. Analyzes were performed on 2 to 3 rats per group and 7 to 15 images per animal were quantified using Image J software (National Institutes of Health, Bethesda, MD). Apoptotic cells were expressed as percentage of nuclear positive red staining per field.

Experimental Procedures

Pressure-Volume Loop Analysis

Animals were deeply anesthetized as previously described. LV pressures and volumes were measured with a pressure-volume conductance catheter (SPR-869, Millar Instruments, Houston, TX) inserted first into the right carotid artery to measure baseline arterial pressure (5-minute record), and then into the LV to record systolic and diastolic hemodynamics. End-systolic-pressure-volume relationship and end-diastolic-pressure-volume relationship were calculated using 5 consecutive cycles following occlusion of the inferior vena cava.

Sympathetic Nervous System Activity

Power spectral analysis of blood pressure variability was carried out using the baseline 5-minute arterial pressure record, before catheter insertion into the LV cavity. Signals were processed using rodent spectral analysis software (SA-BPV, Nevrokard, Ljubljana, Slovenia). Frequency domain analysis of diastolic pressure variability was performed. Power and normalized units of the low frequency (0.25–0.75 Hz) and high frequency (0.75–3 Hz) were computed, as well as the low frequency/high frequency ratio, considered as general marker of sympathovagal balance.

Infarct Size Measurement and Tissue Sampling

After experimental procedures, blood was collected from the inferior vena cava and centrifuged 10 minutes at 4500*g* in order to measure hematocrit. Hearts were excised and sectioned into atria and ventricles. The right ventricle was harvested and the LV was opened from the base to the apex along the middle of the septum and photographed. Infarcted areas were determined as described by Loennechen et al.[22] Then, the LV was divided into infarcted and remote zones. Organs were weighted, rapidly frozen, and kept at –80°C.

Western Blotting

Frozen samples of remote areas were homogenized using mortar and pestle and were lysed to extract total proteins (Precellys 24, 6500 rpm, 3 × 20 seconds–5 seconds, Bertin Technology, Montigny le Bretonneux, France; sample lysis buffer: 5 mmol/L EDTA, 1 mmol/L Na_3VO_4, 20 mmol/L NaF, 1 mmol/L dithiothreitol, and protease inhibitor cocktails) or nuclear proteins (Nuclear Extract Kit; Active Motif Europe, Rixensart, Belgium). The protein concentration was calculated using Bradford assay (Bradford's reagent, Sigma-Aldrich, Saint-Quentin Fallavier, France). Thirty milligrams of protein were separated by SDS polyacrylamide gels (8%–12%) and transferred to polyvinylidene difluoride membranes. Next, membranes were blocked with 5% nonfat milk or BSA in Tris-buffered saline with Tween 20 (0.1%). Membranes were then incubated overnight at 4°C with primary antibodies in Tris-buffered saline-Tween 20 (0.1%), 5% BSA, or nonfat milk. The following day, membranes were incubated for 1 hour at room temperature with the appropriate horseradish peroxidase–conjugated anti-IgG (1: 5000, Santa Cruz Biotechnology, Heidelberg, Germany). Enhanced chemiluminescence was performed with the Western Blot ECL substrate (Clarity; Bio-Rad, Marnes-la Coquette, France) according to the manufacturer's instructions and video acquisition (ChemiDoc-XRS-System, Bio-Rad). The relative

Downloaded from http://ahajournals.org by on October 13, 2022

amount of protein was quantified by densitometry (ImageJ). The following antibodies were used: the transcription factor ATF4, caspase-12, caspase-3, cleaved caspase-3 (1:1000, Cell Signaling Technology, Hitchin, UK), nuclear transcription factor CHOP (C/EBP homologous binding protein), Grp78 (chaperone protein), TBP (TATA binding protein) (1: 1000, Santa Cruz Biotechnology), nuclear HIF-1α (1: 500), and tubulin (1: 2000, Santa Cruz Biotechnology). Phosphorylated proteins were expressed relative to total proteins, and nonphosphorylated cytosolic proteins were expressed relative to tubulin. Nuclear CHOP and HIF-1α were expressed relative to TBP.

RNA Isolation, Reverse Transcription, and Quantitative Real-Time Polymerase Chain Reaction

Total mRNA from remote areas were extracted using RNA isolation kit (Nucleospin RNA Plus, Macherey-Nagel, Düren, Allemagne). Total RNA (0.5 µg) was reversely transcribed to cDNA using iScript Reverse Transcription Supermix (C-1000 Thermal Cycler, Bio-Rad). Quantitative real-time polymerase chain reaction was performed using SsoAdvanced Universal SYBR Green Supermix (Bio-Rad) and polymerase chain reaction primers for Nppa, Nppb, and Acta1 (Sigma-Aldrich). Primer sequences are listed in Table 1. Quantification of mRNA was standardized to the 2 best household genes (Cyca, Rplp0, and HPRT1) selected with the RefFinder program,[23] and was calculated using the 2ΔΔCt method.

Statistical Analysis

Statistical analysis was performed using GraphPad Prism 6 software (San Diego, CA). Data are expressed as means±SEM. For each comparison group, normality and equal variance were tested using Shapiro–Wilk and Bartlett tests, respectively. When these assumptions were met, results were analyzed using 2-way ANOVA, followed by post hoc Sidak's multiple comparison tests. In other conditions and when sample size was too small (n < 3), Kruskal–Wallis test was used, followed by Dunn's multiple comparison test. For ultrasonographic parameters, repeated-measures ANOVA was used (Prism; GraphPad Software, La Jolla, CA). A 2-sided $P < 0.05$ was considered statistically significant.

RESULTS

IH Impacts Heart and Lung Weights and Volumes

IH induced a significant increase in hematocrit compared with Sham and MI-N animals at both 4 and 12 weeks (Table 2). After 12 weeks MI, body weight was lower in MI-IH compared with Sham and MI-N animals ($^{*}P < 0.05$ vs Sham and $^{\dagger}P < 0.05$ vs MI-N; Table 2 and Figure 2A). Heart and LV weights were significantly increased in both MI-N and MI-IH compared with Sham ($^{*}P < 0.05$ vs Sham; Table 1, Figure 2B and 2C), whereas right ventricle and lung weights were significantly increased in the MI-IH group only ($^{*}P < 0.05$ vs Sham and $^{\dagger}P < 0.05$ vs MI-N; Table 2, Figure 2D and 2E).

IH Exacerbates Cardiac Remodeling and Contractile Dysfunction During the Time Course of Ischemic Cardiomyopathy Development

Three days after coronary artery ligation, we validated the surgical procedure homogeneity by echocardiography. After 4 and 12 weeks of exposure to IH or N, infarct sizes were similar between MI-N and MI-IH groups (29±2 vs 29±1% of LV area in N and IH rats, respectively, after 4 weeks MI; and 22±2 vs 23±1% in N and IH, respectively, after 12 weeks; Table 2). At 4 weeks, MI induced LV dilation in both N and IH groups compared with Sham, characterized by increased end-diastolic LV internal diameter (Table 2). This was associated with cardiac dysfunction as shown by significant decreases in LV fractional shortening, dP/dtmax, and dP/dtmin in both MI-N and MI-IH ($P < 0.05$ vs Sham; Table 2) and a decrease in stroke volume and cardiac output (CO) in MI-IH compared to Sham ($P < 0.05$ vs Sham; Table 2). At 12 weeks, our data confirmed the acceleration of cardiac dysfunction in MI-IH compared with MI-N, as

Table 1. Primers Used for RT-qPCR

Genes	Proteins	Forward Primer 5′-3′	Reverse primer 3′-5′
Cyca	Cyclin A	TATCTGCACTGCCAAGACTGAGTG	CTTCTTGCTGGTCTTGCCATTCC
Rplp0	Ribosomal protein large P0	CCCTGCACTCTCGCTTTCTGGA	AGGGGCAGCAGCCGCAAATG
HPRT1	Hypoxanthine phosphorybosyltransferase1	GGGGGACATAAAAGTTATTGGTGGA	GGTCCTTTTCACCAGCAAGCTTG
Nppa	Natriuretic peptide A	AGGCCATATTGGAGCAAATC	CTCCTCCAGGTGGTCTAGCA
Nppb	Natriuretic peptide B	GCTCTCAAAGGACCAAGGC	AACAACCTCAGCCCGTCAC
Acta1	Skeletal alpha actin	GGCTCCCAGCACCATGAAGA	CAGCACGATTGTCGATTGTCG

Downloaded from http://ahajournals.org by on October 13, 2022

Downloaded from http://ahajournals.org by on October 13, 2022

Table 2. Effects of Chronic IH Exposure on Morphometric and Cardiac Parameters

Morphological parameters	4 weeks exposure						12 weeks exposure					
				P Value MI-N	*P* Value MI-IH					*P* Value MI-N	*P* Value MI-IH	
	Sham	MI-N	MI-IH	vs Sham	vs Sham	vs MI-N	Sham	MI-N	MI-IH	vs Sham	vs Sham	vs MI-N
BW, g	407±10	415±7	377±11	0.547	0.063	0.019	583±19	571±23	483±22	0.691	0.0104	0.017
Hematocrit, %	38.7±0.9	39.0±1.2	46.6±1.4	0.872	<0.001	<0.001	40.0±0.6	42.1±0.8	56.7±0.9	0.056	<0.001	<0.001
Infarct size (% of LV)	/	29±2	29±1	/	/	0.818	/	22±2	23±1	/	/	0.919
HW/TL, mg/mm	27±1	34±2	30±1	<0.001	0.022	0.022	30.8±0.9	34.9±1.1	36.1±1.4	0.036	0.0129	0.476
LVW/TL, mg/mm	21±1	28±1	24±1	<0.001	0.045	0.010	24.4±0.8	28.1±0.9	28.0±1.0	0.028	0.0277	0.988
Cardiac ultrasonography												
LVIDd, mm	8±0.2	11±0.2	10±0.1	<0.001	<0.001	0.001	9±0.1	11.6±0.2	11.4±0.2	<0.001	<0.001	0.420
LVIDs, mm	5±0.2	10±0.2	9±0.2	<0.001	<0.001	0.010	5±0.2	10±0.2	10±0.2	<0.001	<0.001	0.845
LVPWd, mm	1.4±0.0	1.1±0.1	1.2±0.0	<0.001	<0.001	0.025	1.3±0.0	1.1±0.0	1.0±0.0	<0.001	<0.001	0.541
LVPWs, mm	2.1±0.0	1.8±0.0	2.0±0.1	<0.001	0.002	<0.001	2.1±0.0	1.7±0.0	1.5±0.0	<0.001	<0.001	0.004
LVFS, %	34±1.0	14±0.0	15±1	<0.001	<0.001	0.753	39±1	13±1	11±1	<0.001	<0.001	0.004
Cardiac catheterization												
HR, bpm	242.5±8.1	237.0±8.1	244.4±15.3	0.999	0.999	0.992	197.5±11.5	212.7±7.0	207.8±6.6	0.583	0.999	0.999
ESP, mm Hg	82.7±4.1	83.6±0.8	82.3±1.9	0.986	0.986	0.986	82.4±3.1	87.2±2.0	84.6±2.8	0.511	0.797	0.797
EDP, mm Hg	8.3±0.8	8.2±0.5	8.9±0.9	0.894	0.878	0.878	8.9±0.8	9.0±0.6	5.5±1.0	0.919	0.027	0.027
ESV, µL	131±14	308±18	231±34	<0.001	0.014	0.036	127±15	392±31	470±36	<0.001	<0.001	0.068
EDV, µL	212±20	364±25	271±36	0.004	0.153	0.064	263±41	461±31	549±35	0.002	0.001	0.144
SV, µL	127±11	114±14	82±9	0.413	0.025	0.116	189±29	132±9	119±5	0.096	0.082	0.642
CO, mL/min	30.9±3.1	27.0±3.2	19.4±1.9	0.343	0.021	0.131	37.8±6.4	28.3±2.4	24.7±1.4	0.251	0.180	0.590
d*P*/d*t*max, mm Hg/s	5339±325	4510±209	4034±116	0.046	0.002	0.173	5285±270	4257±244	4015±219	0.017	0.012	0.544
d*P*/d*t*min, mm Hg/s	−4269±280	−3452±132	−3294±126	0.019	0.006	0.584	−3883±200	−3274±177	−3202±117	0.065	0.065	0.798
EDPVR	0.04±0.00	0.03±0.00	0.05±0.00	0.479	0.583	0.304	0.04±0.01	0.02±0.00	0.02±0.00	0.081	0.081	0.870

Values are mean±SEM; n=7 to 11 per group. bpm indicates beats per minute; BW, body weight; CO, cardiac output; d*P*/d*t*max, maximum first derivative of change in pressure rise with respect to time; d*P*/d*t*min, maximum first derivative of change in pressure fall with respect to time; EDP, end-diastolic pressure; EDPVR, end-diastolic pressure volume relationship; EDV, end-diastolic volume; ESP, end-systolic pressure; ESV, end-systolic volume; HR, heart rate; HW, heart weight; IH, intermittent hypoxia; LVFS, left ventricular fractional shortening; LVIDd, left ventricular internal diameter in diastole; LVIDs, left ventricular internal diameter in systole; LVPWd, left ventricular posterior wall thickness in diastole; LVPWs, left ventricular posterior wall thickness in systole; LVW, left ventricular weight; MI, myocardial infarction; N, normoxia; SV, stroke volume; TL, tibia length.

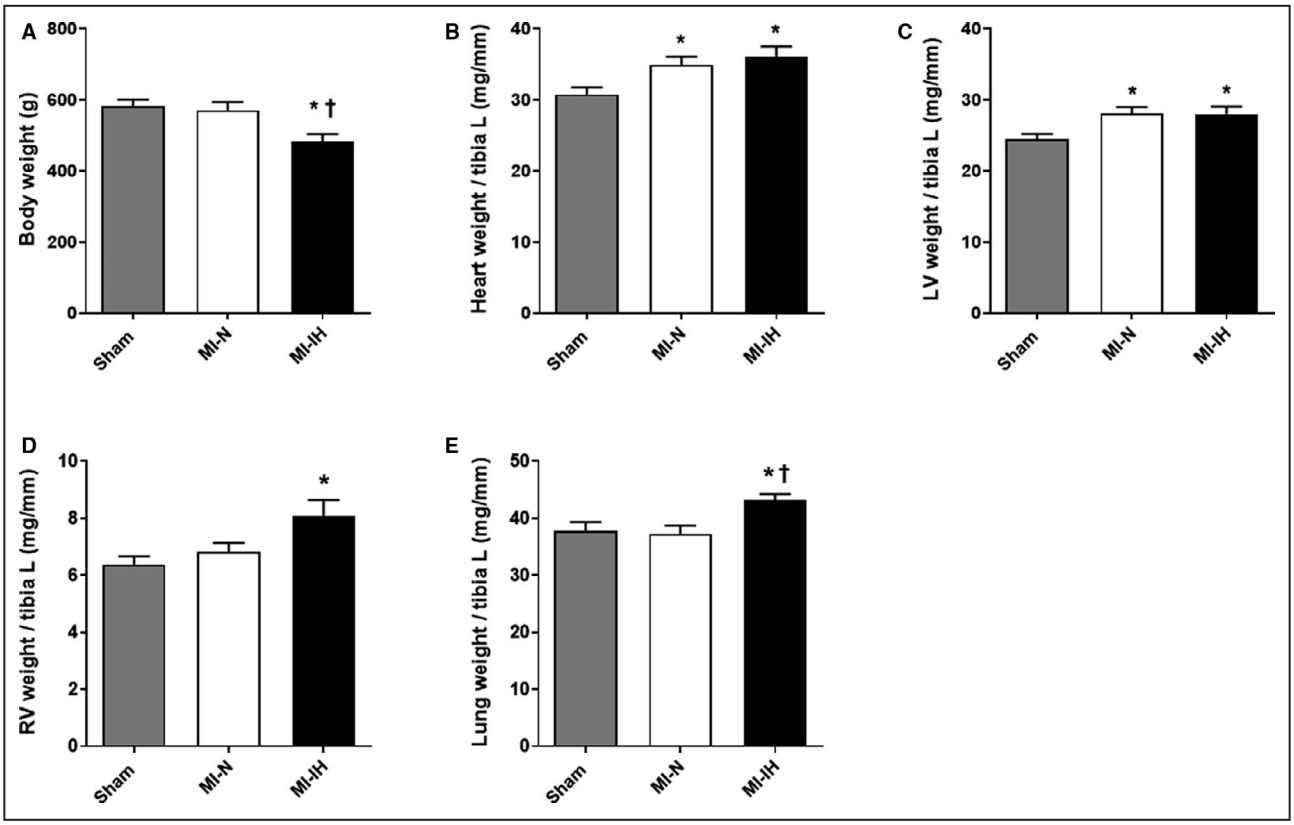

Figure 2. Morphometric parameters after 12 weeks exposure to intermittent hypoxia (IH).
A, Rat body weight. **B**, Heart weight to tibia length (L) ratio. **C**, Left ventricle (LV) weight on tibia length ratio. **D**, Right ventricle (RV) weight on tibia length ratio. **E**, Lung weight on tibia length ratio. Values are mean±SEM. n=7 to 8 per group; *P < 0.05 vs Sham; †P < 0.05 vs MI-N.

revealed by a significantly higher reduction of ejection fraction and end-systolic-pressure-volume relationship compared with MI-N (*P < 0.05 vs Sham and †P < 0.05 vs MI-N; Figure 3A and 3B).

IH Induces LV Remodeling

At 12 weeks, MI induced cardiomyocytes hypertrophy, as shown by the increase in minimum Feret diameter of cardiomyocytes from Sham to MI-N and a maximum increase in MI-IH (*P < 0.05 vs Sham and †P < 0.05 vs MI-N; Figure 4A and 4B). This was associated with dynamic changes in mRNA expression of fetal genes program (Nppa, Nppb, and Acta1) from 4 to 12 weeks (Figure 4C through 4E). In addition, we observed an increase in interstitial fibrosis (*P < 0.05 vs Sham; Figure 4F and 4G) and apoptosis (*P < 0.05 vs Sham; Figure 4H and 4I) in remote LV areas in MI-IH but not in MI-N animals.

IH Induces Sustained Sympathetic Hyperactivity

After 4 weeks of IH, we observed a significant elevation of the low frequency to high frequency (low frequency/high frequency) ratio of diastolic blood pressure variability that lasted until 12 weeks of exposure (*P < 0.05 vs Sham; Figure 5B). As the adrenal medulla releases catecholamines in response to SNS activation, we examined its structural status after 12 weeks. IH rats presented adrenal hypertrophy with a significant increase in adrenal weight to tibia length ratio (*P < 0.05 vs Sham; Figure 5C), associated with significant increase in the medullar area in MI-IH (*P < 0.05 vs Sham; Figure 5E).

IH Induces a Sustained Overexpression of Nuclear HIF-1α Post-MI

After 4-week exposure, nuclear HIF-1α expression was significantly increased in both MI groups, with a more important upregulation in the MI-IH group (*P < 0.05 vs Sham and †P < 0.05 vs MI-N; Figure 6A). At 12 weeks, nuclear HIF-1α expression was normalized to Sham group in MI-N, whereas it remained overexpressed in the MI-IH group over time (*P < 0.05 vs Sham, Figure 6A).

IH Promotes Myocardial Pro-Apoptotic ER Stress

In normoxic animals, MI induced a slight increase in ER stress markers expression over time, with a modest but significant rise in Grp78 expression at both 4

Downloaded from http://ahajournals.org by on October 13, 2022

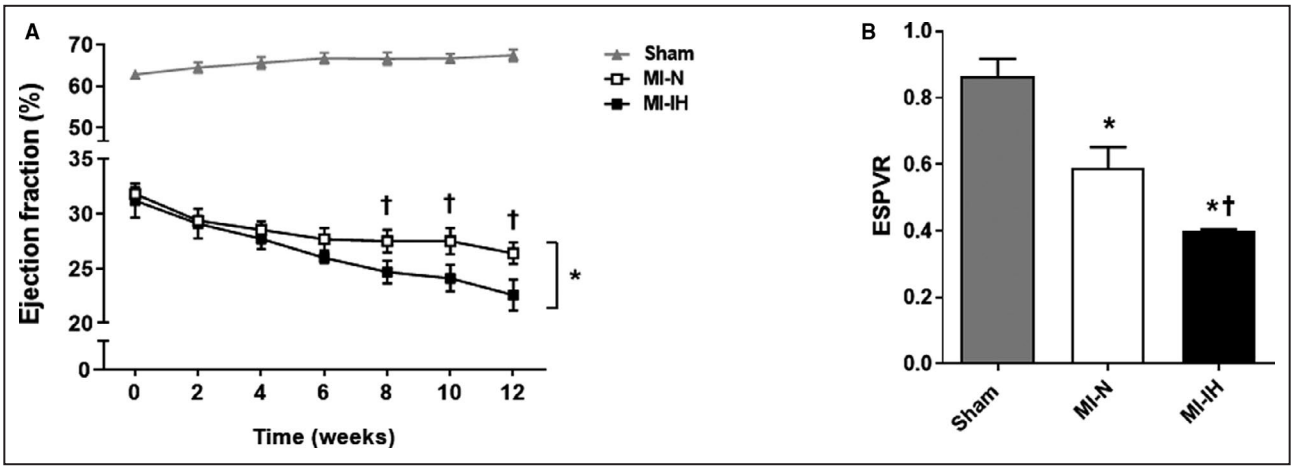

Figure 3. Chronic intermittent hypoxia (IH) precipitates myocardial infarction (MI)-induced contractile dysfunction.
A, Echocardiographic measurement of ejection fraction (EF) over time. **B**, End-systolic pressure-volume relationship (ESPVR) after 12-week exposure to nomoxia (MI-N) or intermittent hypoxia (MI-IH). Values are mean±SEM; n=10 to 11 per group for EF, n=7 to 8 for ESPVR. *P < 0.05 vs Sham and †P < 0.05 vs MI-N.

and 12 weeks (*P < 0.05 vs Sham; Figure 6B). This was associated with a slight increase in the nuclear pro-apoptotic transcription factor CHOP expression and an increase in c-Casp3/Casp3 ratio at 4 weeks, which were no longer elevated at 12 weeks (*P < 0.05 vs Sham; Figure 6D and 6E). ATF4 and Casp12 expressions were not modified in the MI-N group over 12 weeks (Figure 6C and 6F). The kinetic of ER stress markers expression differed in the MI-IH group in which ER stress was limited at 4 weeks compared with Sham and significantly increased at 12 weeks, with a significant increase in Grp78, ATF4, and nuclear CHOP expression (*P < 0.05 vs Sham and †P < 0.05 vs MI-N; Figure 6B through 6D). Interestingly, apoptosis seemed to be present from 4 weeks in the MI-IH group, with increased expression of Casp12 and cCasp3/Casp3, which persisted until 12 weeks (*P < 0.05 vs Sham and †P < 0.05 vs MI-N; Figure 6E and 6F). These results are consistent with TUNEL stainings (Figure 4H and 4I).

DISCUSSION

Our results demonstrate that IH, the hallmark feature of SDB deleterious cardiovascular consequences, precipitates cardiac remodeling and contractile dysfunction during the time course evolution of ischemic cardiomyopathy in rodents. Among associated mechanisms, we identified the early occurrence and persistence of sympathetic activation, associated with sustained nuclear HIF-1α expression and a delayed pro-apoptotic ER stress.

IH Exacerbates the Progression of Ischemic Cardiomyopathy

SDB is highly prevalent in patients with ACS, with a remaining question about the role of chronic IH on long-term prognosis.[24] Application of a positive airway pressure remains the gold standard treatment of SDB. However, although many studies demonstrated the benefit of continuous positive airway pressure on quality of life and neurocognitive dysfunctions,[25] recent large clinical trials reported that continuous positive airway pressure failed to prevent cardiovascular mortality,[26,27] underlying the complex relationship between SDB and cardiovascular complications.[28] In this context, well-controlled animal studies are required to demonstrate the long-term impact of chronic IH on ischemic cardiomyopathy progression

Figure 4. Effect of chronic IH on cardiac remodeling.
A, Representative images of wheat germ agglutinin staining. **B**, Measurement of minimum Feret diameter from Sham, myocardial infarction normoxia (MI-N) and myocardial infarction intermittent hypoxia (MI-IH) rats at 12 weeks intermittent hypoxia or normoxia. Values are mean±SEM; n=2 to 3 animals per group, 100 to 400 cells per animal; *P < 0.05 vs Sham; †P < 0.05 vs MI-N. **C**, Nppa (natriuretic peptide type A), **D**, Nppb (natriuretic peptide type B), **E**, actin alpha1 skeletal muscle (Acta1) mRNA expression relative to household genes mRNA expression at 4- and 12-weeks experiment. Values are normalized to Sham group (dashed line) and expressed as mean±SEM. n=7 to 8 per group; *P < 0.05 vs Sham. **F**, Representative images of Sirius red staining. **G**, Interstitial fibrosis evaluated in the LV remote area as a percentage of Sirius red staining relative to cardiomyocytes area, in myocardium from Sham, MI-N, and MI-IH rats at 12 weeks experiment. Values are mean±SEM; n=2 to 3 animals per group, 20 to 40 images per animal; *P < 0.05 vs Sham. **H**, Representative images of TUNEL staining. I. Apoptotic cells quantified in the LV remote area and expressed as percentage of nuclear positive red staining per field. Values are mean±SEM; n=2 to 3 animals per group, 7 to 15 images per animal; *P < 0.05 vs Sham. LV indicates left ventricular.

Downloaded from http://ahajournals.org by on October 13, 2022

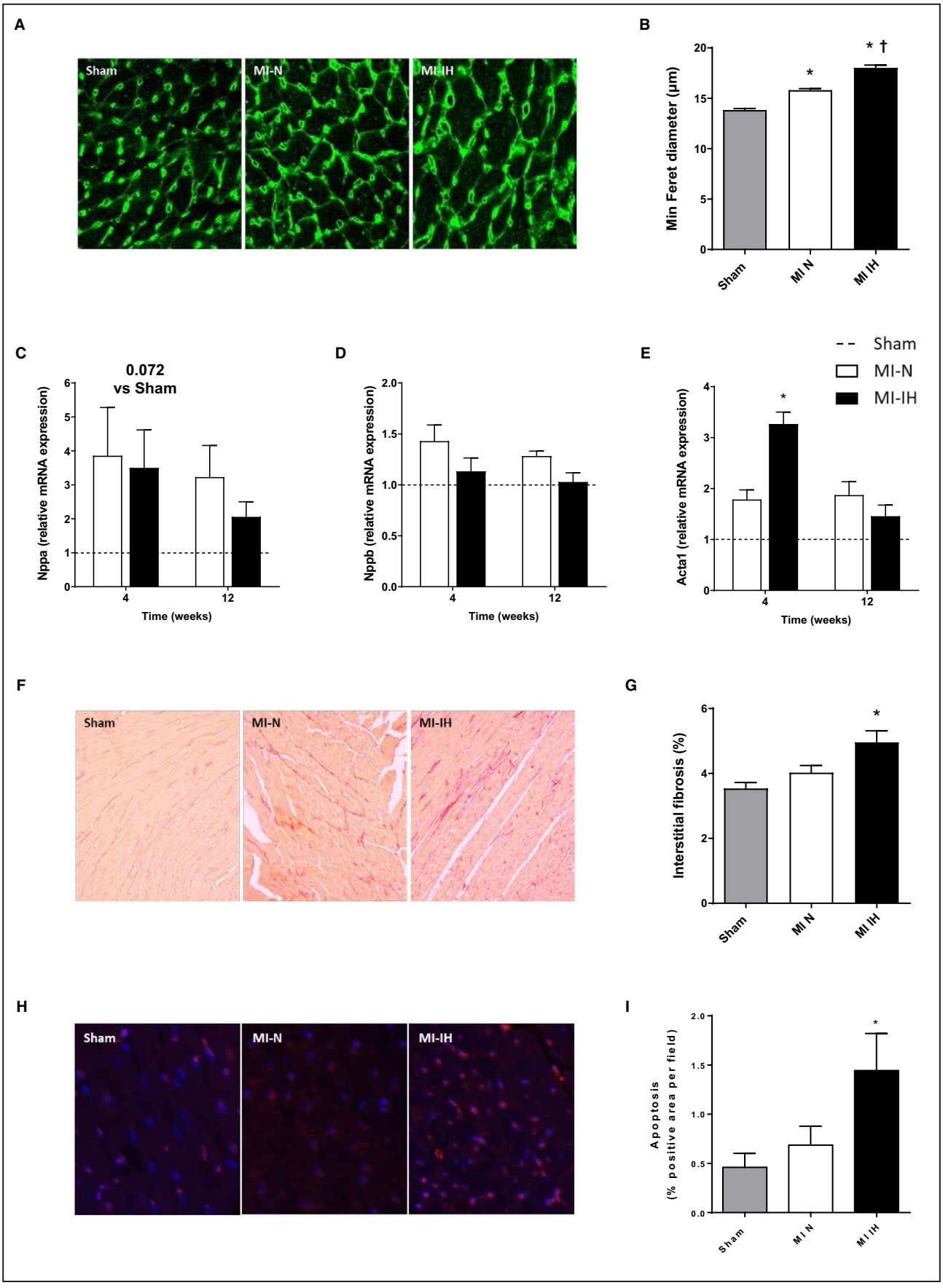

Downloaded from http://ahajournals.org by on October 13, 2022

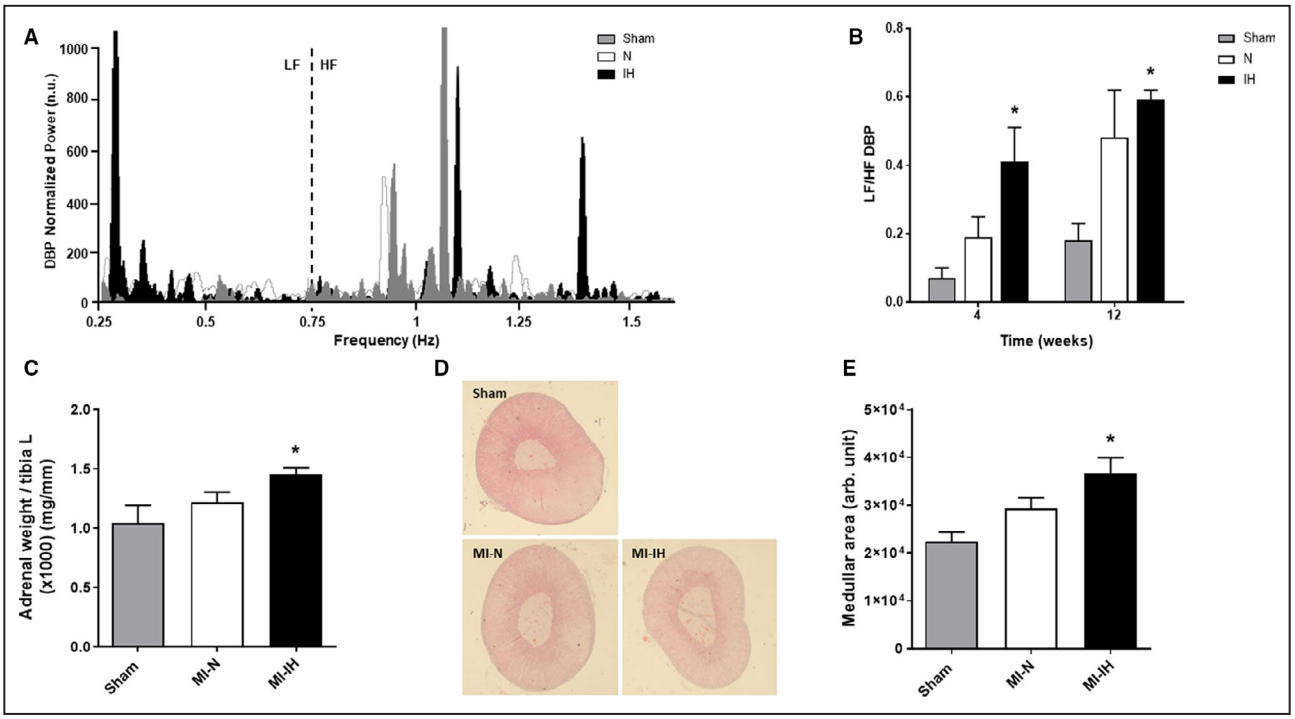

Figure 5. Chronic intermittent hypoxia (IH) exposure increases sympathetic activity post-myocardial infarction (MI). **A**, Representative power analysis spectra of diastolic blood pressure (DBP) variability from sham animals or rats with MI exposed to normoxia (N) or intermittent hypoxia (IH). **B**, Quantification of low-frequency-to-high-frequency ratio from DBP variability (LF/HF DBP) after 4- and 12-week exposure to N or IH in MI and Sham rats. **C**, Adrenal hypertrophy measured by adrenal weight to tibia length (L) ratio. **D**, Representative images of adrenal gland sections from Sham, MI-N, and MI-IH animals. **E**, Medulla area in arbitrary units (arb. unit). Values are mean±SEM; n=7 to 8 per group; **P* < 0.05 vs Sham. n.u. indicates normalized unit.

and to decipher associated mechanisms. This would allow proposing new therapeutic targets, and even potential biomarkers of disease severity, in order to improve management of SDB-related cardiovascular risk in patients with ischemic cardiomyopathy, in addition to continuous positive airway pressure. The originality of our data is to make available a sequential long-term longitudinal echocardiographic follow-up. At 4 weeks of IH, cardiac remodeling did not significantly differ between MI-N and MI-IH rats. However, at the functional level, although the decrease in ejection fraction induced by coronary ligation was identical in the MI-IH and MI-N groups, the reduction of cardiac output was more pronounced in the IH group. In the long term, cardiac function started to decline after 6 weeks of IH exposure with, at 12 weeks, a significantly higher reduction in end-systolic-pressure-volume relationship and ejection fraction in the MI-IH group compared with the MI-N group. This was associated with LV cardiomyocyte hypertrophy and interstitial fibrosis. Such a marked LV remodeling and dysfunction in MI-IH animals was associated with right ventricle hypertrophy and lung edema, confirming an accelerated progression of ischemic cardiomyopathy to heart failure after long-term IH exposure.

IH Induces an Early and Sustained Sympathetic Hyperactivity

Following myocardial ischemia, SNS is activated as a compensatory mechanism in order to increase contractile performance and maintain cardiac output. However, sustained and persistent SNS stimulation in turn drives a maladaptive response, through desensitization of adrenergic signaling, direct effects on cardiomyocytes (ie, apoptosis, hypertrophy, and interstitial fibrosis) and a subsequent and progressive reduction of cardiac output.[29] In the present study, we demonstrated that IH induced an early and persistent sympathetic activity over time. Interestingly, spectral analysis of blood pressure was realized 12 hours after the last IH exposure, indicating that sympathetic activation persists after cessation of IH stimulus in accordance with data in patients with SDB.[25] At 4 weeks IH exposure, the increase in low frequency/high frequency ratio preceded cardiac remodeling and severe contractile dysfunction, acting as a compensatory mechanism. This is in accordance with previous data demonstrating that 4 weeks of IH exposure in C57BL/6J mice increases cardiac contractility through activation of cardiac β-adrenergic pathways.[30] On the other hand, such a sustained sympathetic activity in the long term

Downloaded from http://ahajournals.org by on October 13, 2022

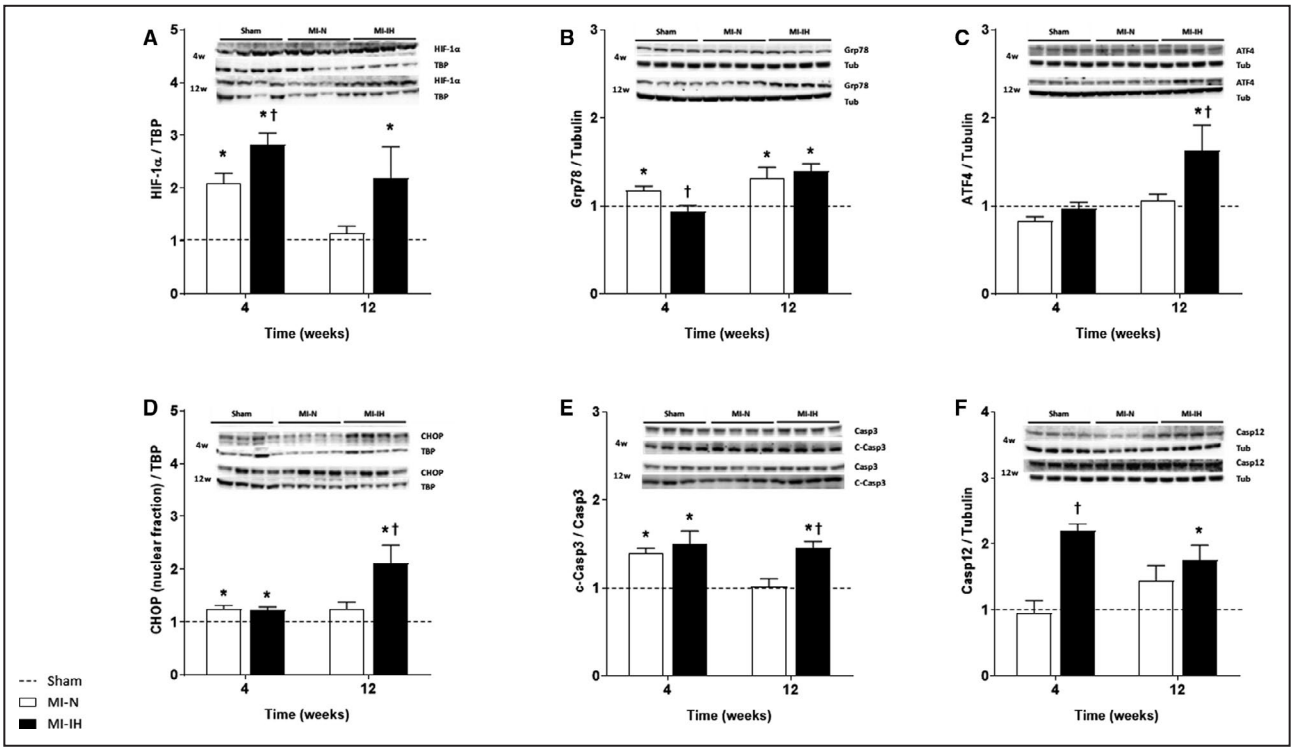

Figure 6. Effect of myocardial infarction (MI) and intermittent hypoxia (IH) exposure on myocardial hypoxia-inducible factor-1α (HIF-1α) expression, endoplasmic reticulum (ER) stress, and apoptosis.
A, Nuclear HIF-1α expression relative to TBP (TATA binding protein). **B**, Grp-78 (glucose-regulated protein kinase) expression relative to tubulin. **C**, Activating transcription factor (ATF)-4 expression relative to tubulin. **D**, Nuclear CHOP (C/EBP homologous binding protein) expression relative to TBP. **E,** Cleaved-caspase 3 (C-Casp3) expression relative to caspase 3 (Casp3). **F**, Caspase 12 (Casp12) expression relative to tubulin. Values are normalized to sham group (dashed line) and expressed as mean±SEM. n=7 to 8 per group; $^{*}P < 0.05$ vs Sham; $^{\dagger}P < 0.05$ vs MI-normoxia (N).

might be responsible for the cardiac remodeling and contractile dysfunction we observed in the MI-IH group between 6 and 12 weeks.

IH Induces Sustained Nuclear HIF-1 Expression

We have previously demonstrated that chronic exposure to IH induces a sustained activation of HIF-1[31] responsible for the increased infarct size.[11] Here, we demonstrated that cardiac HIF-1α nuclear expression was elevated at 4 weeks in both MI-N and MI-IH animals. However, whereas expression was normalized at 12 weeks in MI-N rats, HIF-1α nuclear expression remains elevated at 12 weeks in MI-IH, reflecting the sustained and persistent activation only within IH animals. Previous studies have highlighted that long-term HIF-1α stabilization triggers the development of cardiomyopathy in rodents.[32,33] Indeed, mice with inducible cardiomyocyte-specific expression of HIF-1α exhibited a progressive decrease in cardiac function concomitantly with transgene expression.[33] In addition, constitutive cardiac-specific HIF-1 overexpression in mice mediates beneficial effects in the short term, whereas it triggers cardiac dysfunction occurrence with aging.[32] Finally, in patients with cardiomyopathy, HIF-1α expression is increased in heart samples[32] and high plasmatic HIF-1α level correlates with a decrease in ejection fraction and survival rate in patients with decompensated heart failure.[34]

IH Induces Late Pro-Apoptotic ER Stress

ER stress plays a major role in development of cardiovascular diseases.[35] ER stress, characterized by an increase in CHOP expression, contributes to cardiac apoptosis, hypertrophy, and contractile dysfunction in rodent models of pressure overload.[36,37] In the current study, we determined pro-apoptotic ER stress at 12 weeks only in the MI-IH group, which was concomitant with the progression of ischemic cardiomyopathy to heart failure. These results are in line with previous studies demonstrating that, independently of MI, IH induces deleterious pro-apoptotic ER stress in myocardium.[11,12,15,16] Indeed, tauroursodeoxycholic acid, an ER stress inhibitor, prevents the IH-induced increase in infarct size[11] and several cardioprotective strategies, such as adiponectin,[16] metallothionein,[15] and high-intensity exercise,[12] limit the IH-induced myocardial pro-apoptotic ER stress and associated decline in cardiac function.

Downloaded from http://ahajournals.org by on October 13, 2022

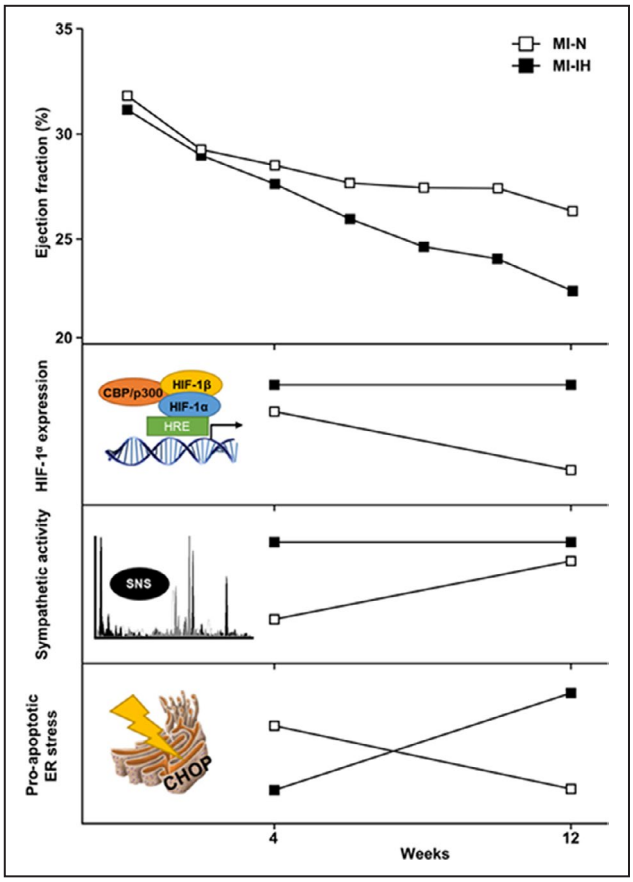

Figure 7. Schematic representation of intermittent hypoxia-induced cardiac dysfunction and associated mechanisms time-course in a rat model of ischemic cardiomyopathy.
CBP indicates CREB binding protein; CHOP, C/EBP homologous protein; ER, endoplasmic reticulum; HIF-1α, hypoxia-inducible factor-1α; HRE, hypoxia response element; MI-IH, myocardial infarction-intermittent hypoxia; MI-N, myocardial infarction normoxia; SNS, sympathetic nervous system.

Interconnection Between IH-Induced Mechanisms

A crosstalk between mechanisms reported above is supported by the literature. In mice, HIF-1α deletion prevents the IH-induced sympathetic activity[38] and recent evidence suggests that, during hypoxia, sympathetic activation increases HIF-1α expression and stabilization in kidney.[39] Adrenergic stimulation also induces cardiac ER stress and subsequent cardiac dysfunctions,[40,41] while β-blockers are able to reduce pro-apoptotic ER stress in a dog model of ischemic cardiomyopathy.[42] Finally, IH-induced cardiac ER stress activates HIF-1, initiating a vicious circle as HIF-1 triggers ER stress and CHOP-mediated apoptosis in alveolar epithelial cells.[43] In our study, the time course of IH effects starts with a concomitant sympathetic overactivity and nuclear HIF-1 expression, which might trigger mechanisms of IH-induced accelerated cardiac remodeling and post-MI dysfunction, whereas ER stress activation occurs later with the decline of cardiac function (Figure 7).

CONCLUSIONS

We have described for the first time the different steps and possible mechanisms associating IH and accelerated deterioration in cardiac function post-MI. Further studies are needed to evaluate whether targeting IH-induced SNS or HIF1 overactivities could limit these effects and improve management of coexisting ischemic cardiomyopathy and SDB.

Study Limitations

1. Whereas we demonstrated the deleterious impact of IH on post-MI cardiac remodeling and contractile dysfunction, associated with activation of several mechanisms (SNS activation, HIF-1 nuclear expression, and pro-apoptotic ER stress), our present study cannot make a firm conclusion on the specific role of each one. Importantly, all these mechanisms could be interconnected, and further studies are needed to establish their respective contributions to IH-induced post-MI dysfunctions.
2. SDB exhibits a complex pathophysiology. Apart from IH, which is described as the main contributor to cardiovascular complications, SDB are also associated with sleep fragmentation and intrathoracic pressure swings and we cannot exclude their contributions on post-MI cardiac remodeling and decline in cardiac function.

ARTICLE INFORMATION

Received February 24, 2020; accepted June 30, 2020.

Affiliations

From the Univ. Grenoble Alpes, INSERM, CHU Grenoble Alpes, HP2, Grenoble, France.

Acknowledgments

We are grateful to Dr Jonathan Gaucher for his ideas about the conclusion figure.

Sources of Funding

This work was supported by the Fond de dotation Agir Pour les Maladies Chroniques (France), Institut National de la Sante et de la Recherche (France) and Université Grenoble Alpes (France). Maximin Détrait is recipient of a PhD fellowship from Société Française de Recherche et Médecine du Sommeil (France).

Disclosures

None.

REFERENCES

1. GBD 2013 Mortality and Causes of Death Collaborators. Global, regional, and national age-sex specific all-cause and cause-specific mortality for 240 causes of death, 1990–2013: a systematic analysis for the Global Burden of Disease Study 2013. *Lancet Lond Engl*. 2015;385:117–171.

Downloaded from http://ahajournals.org by on October 13, 2022

2. Kristian T, Alpert JS, Jaffe AS, Simoons ML, Chaitman BR, White HD. Third universal definition of myocardial infarction.F *Circulation*. 2012;126:2020–2035.
3. Velagaleti RS, Pencina MJ, Murabito JM, Wang TJ, Parikh NI, D'Agostino RB, Levy D, Kannel WB, Vasan RS. Long-term trends in the incidence of heart failure after myocardial infarction. *Circulation*. 2008;118:2057–2062.
4. Gottlieb DJ, Yenokyan G, Newman AB, O'Connor GT, Punjabi NM, Quan SF, Redline S, Resnick HE, Tong EK, Diener-West M, et al. Prospective study of obstructive sleep apnea and incident coronary heart disease and heart failure. *Circulation*. 2010;122:352–360.
5. Ludka O, Stepanova R, Vyskocilova M, Galkova L, Mikolaskova M, Belehrad M, Kostalova J, Mihalova Z, Drozdova A, Hlasensky J, et al. Sleep apnea prevalence in acute myocardial infarction–the Sleep Apnea in Post-acute Myocardial Infarction Patients (SAPAMI) Study. *Int J Cardiol*. 2014;176:13–19.
6. Khayat R, Jarjoura D, Porter K, Sow A, Wannemacher J, Dohar R, Pleister A, Abraham WT. Sleep disordered breathing and post-discharge mortality in patients with acute heart failure. *Eur Heart J*. 2015;36:1463–1469.
7. Buchner S, Satzl A, Debl K, Hetzenecker A, Luchner A, Husser O, Hamer OW, Poschenrieder F, Fellner C, Zeman F, et al. Impact of sleep-disordered breathing on myocardial salvage and infarct size in patients with acute myocardial infarction. *Eur Heart J*. 2014;35:192–199.
8. Barbé F, Sánchez-de-la-Torre A, Abad J, Durán-Cantolla J, Mediano O, Amilibia J, Masdeu MJ, Florés M, Barceló A, de la Peña M, et al. Effect of obstructive sleep apnoea on severity and short-term prognosis of acute coronary syndrome. *Eur Respir J*. 2015;45:419–427.
9. Dematteis M, Godin-Ribuot D, Arnaud C, Ribout C, Stanke-Labesque F, Pépin J, Lévy P. Cardiovascular consequences of sleep-disordered breathing: Contribution of animal models to understanding of the human disease. *Ilar J*. 2009;50:262–281.
10. Park A-M, Suzuki YJ. Effects of intermittent hypoxia on oxidative stress-induced myocardial damage in mice. *J Appl Physiol*. 2007;102:1806–1814.
11. Belaidi E, Thomas A, Bourdier G, Moulin S, Lemarié E, Levy P, Pépin JL, Korichneva I, Godin-Ribuot D, Arnaud C. Endoplasmic reticulum stress as a novel inducer of hypoxia inducible factor-1 activity: Its role in the susceptibility to myocardial ischemia-reperfusion induced by chronic intermittent hypoxia. *Int J Cardiol*. 2016;210:45–53.
12. Bourdier G, Flore P, Sanchez H, Pepin J-L, Belaidi E, Arnaud C. High-intensity training reduces intermittent hypoxia-induced ER stress and myocardial infarct size. *Am J Physiol-Heart Circ Physiol*. 2016;310:H279–H289.
13. Lai CJ, Yang CCH, Hsu YY, Lin YN, Kuo TBJ. Enhanced sympathetic outflow and decreased baroreflex sensitivity are associated with intermittent hypoxia-induced systemic hypertension in conscious rats. *J Appl Physiol*. 2006;100:1974–1982.
14. Morand J, Arnaud C, Pepin J-L, Godin-Ribuot D. Chronic intermittent hypoxia promotes myocardial ischemia-related ventricular arrhythmias and sudden cardiac death. *Sci Rep*. 2018;8:2997.
15. Zhou S, Yin X, Zheng Y, Miao X, Feng W, Cai J, Cai L. Metallothionein prevents intermittent hypoxia-induced cardiac endoplasmic reticulum stress and cell death likely via activation of Akt signaling pathway in mice. *Toxicol Lett*. 2014;227:113–123.
16. Ding W, Zhang X, Huang H, Ding N, Zhang S, Hutchinson SZ, Zhang X. Adiponectin protects rat myocardium against chronic intermittent hypoxia-induced injury via inhibition of endoplasmic reticulum stress. *PLoS One*. 2014;9:e94545.
17. Chou Y-T, Zhan G, Zhu Y, Fenik P, Panossian L, Li Y, Zhang J, Veasey S. C/EBP homologous binding protein (CHOP) underlies neural injury in sleep apnea model. *Sleep*. 2013;36:481–492.
18. Belaidi E, Morand J, Gras E, Pépin J-L, Godin-Ribuot D. Targeting the ROS-HIF-1-endothelin axis as a therapeutic approach for the treatment of obstructive sleep apnea-related cardiovascular complications. *Pharmacol Ther*. 2016;168:1–11.
19. Litwin SE, Katz SE, Morgan JP, Douglas PS. Serial echocardiographic assessment of left ventricular geometry and function after large myocardial infarction in the rat. *Circulation*. 1994;89:345–354.
20. Arnaud C, Beguin PC, Lantuejoul S, Pepin J-L, Guillermet C, Pelli G, Burger F, Buatois V, Ribuot C, Baguet J-P, et al. The inflammatory preatherosclerotic remodeling induced by intermittent hypoxia is attenuated by RANTES/CCL5 inhibition. *Am J Respir Crit Care Med*. 2011;184:724–731.
21. Moulin S, Arnaud C, Bouyon S, Pépin J-L, Godin-Ribuot D, Belaidi E. Curcumin prevents chronic intermittent hypoxia-induced myocardial injury. *Ther Adv Chronic Dis*. 2020;11:2040622320922104. https://doi.org/10.1177/2040622320922104.
22. Loennechen JP, Støylen A, Beisvag V, Wisløff U, Ellingsen O. Regional expression of endothelin-1, ANP, IGF-1, and LV wall stress in the infarcted rat heart. *Am J Physiol Heart Circ Physiol*. 2001;280:H2902–H2910.
23. Xie F, Xiao P, Chen D, Xu L, Zhang B. miRDeepFinder: a miRNA analysis tool for deep sequencing of plant small RNAs. *Plant Mol Biol*. 2012;80:75–84.
24. Randerath W, Bonsignore MR, Herkenrath S. Obstructive sleep apnoea in acute coronary syndrome. *Eur Respir Rev*. 2019;28:180114.
25. Lévy P, Kohler M, McNicholas WT, Barbé F, McEvoy RD, Somers VK, Lavie L, Pépin JL. Obstructive sleep apnoea syndrome. *Nat Rev Dis Primer*. 2015;1:15015.
26. Sánchez-de-la-Torre Manuel, Sánchez-de-la-Torre Alicia, Bertran Sandra, Abad Jorge, Duran-Cantolla Joaquín, Cabriada Valentín, Mediano Olga, Masdeu María José, Alonso Mari Luz, Masa Juan Fernando, et al. Effect of obstructive sleep apnoea and its treatment with continuous positive airway pressure on the prevalence of cardiovascular events in patients with acute coronary syndrome (ISAACC study): a randomised controlled trial. *The Lancet Respiratory Medicine*. 2020;8:359–367. http://dx.doi.org/10.1016/s2213-2600(19)30271-1.
27. McEvoy RD, Antic NA, Heeley E, Luo Y, Ou Q, Zhang X, Mediano O, Chen R, Drager LF, Liu Z, et al. CPAP for prevention of cardiovascular events in obstructive sleep apnea. *N Engl J Med*. 2016;375:919–931.
28. Heinzer Raphael, Eckert Danny. Treatment for obstructive sleep apnoea and cardiovascular diseases: are we aiming at the wrong target? *The Lancet Respiratory Medicine*. 2020;8:323–325. http://dx.doi.org/10.1016/s2213-2600(19)30351-0.
29. El-Armouche A, Eschenhagen T. β-Adrenergic stimulation and myocardial function in the failing heart. *Heart Fail Rev*. 2009;14:225–241.
30. Naghshin J, McGaffin KR, Witham WG, Mathier MA, Romano LC, Smith SH, Janczewski AM, Kirk JA, Shroff SG, O'Donnell CP. Chronic intermittent hypoxia increases left ventricular contractility in C57BL/6J mice. *J Appl Physiol*. 2009;107:787–793.
31. Belaidi E, Joyeux-Faure M, Ribuot C, Launois SH, Levy P, Godin-Ribuot D. Major role for hypoxia inducible factor-1 and the endothelin system in promoting myocardial infarction and hypertension in an animal model of obstructive sleep apnea. *J Am Coll Cardiol*. 2009;53:1309–1317.
32. Hölscher M, Schäfer K, Krull S, Farhat K, Hesse A, Silter M, Lin Y, Pichler BJ, Thistlethwaite P, El-Armouche A, et al. Unfavourable consequences of chronic cardiac HIF-1α stabilization. *Cardiovasc Res*. 2012;94:77–86.
33. Bekeredjian R, Walton CB, MacCannell KA, Ecker J, Kruse F, Outten JT, Sutcliffe D, Gerard RD, Bruick RK, Shohet RV. Conditional HIF-1α expression produces a reversible cardiomyopathy. *PLoS One*. 2010;5:1–11.
34. Li G, Lu W, Wu X, Cheng J, Ai R, Zhou Z, Tang Z. Admission hypoxia-inducible factor 1α levels and in-hospital mortality in patients with acute decompensated heart failure. *BMC Cardiovasc Disord*. 2015;15:79.
35. Groenendyk J, Agellon LB, Michalak M. Coping with endoplasmic reticulum stress in the cardiovascular system. *Annu Rev Physiol*. 2013;75:49–67.
36. Fu HY, Okada K-I, Liao Y, Tsukamoto O, Isomura T, Asai M, Sawada T, Okuda K, Asano Y, Sanada S, et al. Ablation of C/EBP homologous protein attenuates endoplasmic reticulum-mediated apoptosis and cardiac dysfunction induced by pressure overload. *Circulation*. 2010;122:361–369.
37. Yao Y, Lu Q, Hu Z, Yu Y, Chen Q, Wang QK. A non-canonical pathway regulates ER stress signaling and blocks ER stress-induced apoptosis and heart failure. *Nat Commun*. 2017;8:133.
38. Peng YJ, Yuan G, Ramakrishnan D, Sharma SD, Bosch-Marce M, Kumar GK, Semenza GL, Prabhakar NR. Heterozygous HIF-1α deficiency impairs carotid body-mediated systemic responses and reactive oxygen species generation in mice exposed to intermittent hypoxia. *J Physiol*. 2006;577:705–716.
39. Cheong HI, Asosingh K, Stephens OR, Queisser KA, Xu W, Willard B, Hu B, Dermawan JKT, Stark GR, Prasad SVN, et al. Hypoxia sensing through β-adrenergic receptors. *JCI Insight*. 2016;1:21. http://dx.doi.org/10.1172/jci.insight.90240.
40. Zhuo X-Z, Wu Y, Ni Y-J, Liu J-H, Gong M, Wang X-H, Wei F, Wang T-Z, Yuan Z, Ma A-Q, et al. Isoproterenol instigates cardiomyocyte apoptosis and heart failure via AMPK inactivation-mediated endoplasmic reticulum stress. *Apoptosis Int J Program Cell Death*. 2013;18:800–810.

Downloaded from http://ahajournals.org by on October 13, 2022

41. Dalal S, Foster CR, Das BC, Singh M, Singh K. β-Adrenergic receptor stimulation induces endoplasmic reticulum stress in adult cardiac myocytes: role in apoptosis. *Mol Cell Biochem*. 2012;364:59–70.
42. George I, Sabbah HN, Xu K, Wang N, Wang J. β-Adrenergic receptor blockade reduces endoplasmic reticulum stress and normalizes calcium handling in a coronary embolization model of heart failure in canines. *Cardiovasc Res*. 2011;91:447–455.
43. Delbrel E, Soumare A, Naguez A, Label R, Bernard O, Bruhat A, Fafournoux P, Tremblais G, Marchant D, Gille T, et al. HIF-1α triggers ER stress and CHOP-mediated apoptosis in alveolar epithelial cells, a key event in pulmonary fibrosis. *Sci Rep*. 2018;8:1–14.

Downloaded from http://ahajournals.org by on October 13, 2022